journal

J. Am. Ceram. Soc., 73 [10] 3026–32 (1990)

Electrical Properties of Individual Zinc Oxide Grain Boundaries Determined by Spatially Resolved Tunneling Spectroscopy

Gregory S. Rohrer*,† and Dawn A. Bonnell*

Department of Materials Science and Engineering, The University of Pennsylvania, Philadelphia, Pennsylvania 19104

Scanning tunneling microscopy (STM) and spatially resolved tunneling spectroscopy (TS) were used to observe correlations between the geometric structure and electrical properties of polycrystalline ZnO surfaces under ultrahigh vacuum. Constant current images revealed crystallographic features at a range of length scales, including facets which are hundreds of nanometers long and monoatomic steps ≈0.5 nm (≈5 Å) in height. Tunneling spectroscopy was used to identify individual ZnO grains, grain boundaries, and surface impurities. Areas of reduced conductivity which extend 5 to 40 nm (50 to 400 Å) on either side of the grain boundaries are attributed to associated space charge regions. This paper demonstrates that, when used together, STM and TS are powerful techniques for the study of the structure and electrical properties of single interfaces and grain boundaries. [Key words: grain boundaries, zinc oxide, varistors, scanning tunneling microscopy, tunneling.]

I. Introduction

THE elucidation of the mechanisms by which grain boundaries and interfaces affect the bulk properties of polycrystalline materials is a fundamental problem in the design and synthesis of new materials. Although experimental techniques have been developed to probe the composition and structure of some grain boundaries, it is still difficult to probe bonding and electrical phenomena at individual interfaces. The only known experimental technique that is capable of directly probing electrical phenomena at sufficiently high resolution is scanning tunneling microscopy (STM) and tunneling spectroscopy (TS). Since their invention in 1982,[1] these techniques have been successfully used to characterize the structure and electrical properties of a large number of well-defined surfaces.[2–4] STM investigations of polycrystalline and composite surfaces, however, have been much less numerous.[5–10] This is due, at least in part, to the fact that images produced from such materials are more difficult to interpret, because contrast in an STM image can arise from both geometric and electronic effects. For example, an STM image of a flat, homogeneous, crystalline surface is to first approximation a map of constant state density, whereas the image of an inhomogeneous surface can contain contributions from local variations in state density, as well as tunnel barrier, or surface topography. Thus, it is necessary to measure local variations in the tunnel barrier and state density to determine if the source of contrast in STM images of inhomogeneous surfaces is geometric or electronic.

In this paper, we report measurements performed on a polycrystalline semiconductor, zinc oxide (ZnO), which is used commercially as a varistor material. This is an excellent material with which to test the power of spatially resolved tunneling spectroscopy, because the varistor effect is thought to be caused (in part) by an interfacial electrical phenomenon. Bismuth oxide (Bi_2O_3), generally added to these materials to enhance the varistor properties, is insoluble in ZnO and is known to segregate to the grain boundaries. It is thought that the bismuth segregation creates a negatively charged layer in the grain boundary which bends the bands of the adjacent ZnO crystals upward, creating a depletion layer and thus increasing the interfacial resistance.[11] To probe this phenomenon, we have employed an imaging technique in which a series of tunneling spectra are obtained during the imaging process so that features on the images can be correlated to measurements of the local density of states. In some cases, depressed regions observed on STM topographs correlate with regions of reduced conductivity and are, therefore, likely to be grain boundaries.

II. Experimental Procedure

Sintered ZnO with additions of 0.1 mol% manganese oxide (MnO), 0.1 mol% cobalt oxide (CoO), 0.1 mol% Bi_2O_3, and 150 ppm aluminum oxide (Al_2O_3) was prepared by a previously described method.[12] A wafer ≈2 mm thick was cut with a diamond wheel saw and then polished with 0.25-mm diamond paste. After ultrasonic cleaning with acetone and then ethanol, the sample was heated in air at 140°C for 30 min and then at 500°C for 30 min. Although the surface conductivity of the sample following this treatment was insufficient for the tunneling experiment, it increased to acceptable levels after evacuation of the STM chamber. Interestingly, the sample remained conductive for an extended period of time (at least several days) after venting the chamber to air so that results could be obtained in ambient atmospheres and compared with those acquired at ultrahigh vacuum (UHV). The effect of the exposure of these samples to atmospheric gases will be discussed in a forthcoming paper.[13]

The microscope, which is of a standard design and described elsewhere,[9] was attached to an UHV chamber with a base pressure of less than $\approx 2.6 \times 10^{-8}$ Pa (2×10^{-10} torr). Mechanically formed platinum tips were cleaned by field emission or continuous scanning. The sample was heated in situ at 400°C for 10 min to remove chemisorbed gases from the surface. Auger electron spectroscopy analysis of the samples following this treatment (and the transfer of the sample through air to a second chamber) indicated that the surface was contaminated with carbon (≈18 at.%). This level of carbon

L. Levinson—contributing editor

Manuscript No. 197667. Received April 6, 1990; approved June 15, 1990.
Supported by the U.S. Department of Energy, Office of Basic Energy Science under Contract No. FE-FG02-90ER-45428.
*Member, American Ceramic Society.
†Current address: Department of Metallurgical Engineering and Materials Science, Carnegie Mellon University, Pittsburgh, PA 15213.

contamination had to be tolerated, because more vigorous heat treatments that effectively removed carbon from the sample surface also segregated bismuth to the surface of the ZnO grains.

Images were made in the constant current mode (0.2 to 5 nA) at −3-V sample bias, and current–voltage (I–V) curves were acquired at preselected locations on the image during the scanning. When the tip reached one of the selected locations, the feedback loop was momentarily disabled and the current was recorded while the sample bias was ramped linearly from −3.0 to 3.0 V in less than 100 ms. After a brief stabilization interval, the process was repeated 9 more times so that the result for each location is the average of 10 curves. After the image was recorded, each I–V curve could be correlated to a specific point on the image. In each case, the dimensionless quantity $(di/dv)/(i/v)$, which has been demonstrated to be related to the local density of states,[14] was obtained by numerically differentiating the experimentally determined current. When the current decreased to below the detectable limit, at biases near zero, the conductivity was defined to equal zero and the quantity $(di/dv)/(i/v)$ was defined to equal one. This limited dynamic range of the current data was a problem which is nearly always encountered when spectroscopy is performed at a fixed sample-tip separation. However, because $(di/dv)/(i/v)$ is nearly independent of sample-tip separation,[15] it was possible to increase the dynamic range of the spectroscopy data by ramping the tip closer to the sample as the bias is decreased.[‡,16] Instrumental limitations prevented the use of this method while in the imaging mode; however, measurements made using this technique while not imaging are also presented here to aid in the interpretation of the spectra acquired at fixed sample-tip separation.

The logarithmic dependence of the current on sample-tip separation was verified using an interrupted-feedback technique similar to the one used to acquire the I–V curves. In this case, after disabling the feedback circuit, the tip was pulled 1.5 nm (15 Å) away and then ramped toward the sample while measuring the current and maintaining a constant bias. Measurements performed under UHV on the cleaned surface indicated that tunneling occurred through a barrier approximately 4.0 eV high at a range of sample-tip separations 0.7 to 1 nm (7 to 10 Å) wide.[¶] Possible local variations in the tunnel barrier height were not explored at this time.

III. Results

Large field-of-view constant current images often contained faceted features such as those shown in Figs. 1(A) and (B). Note in particular the angles between the edges of the feature in Fig. 1(B) which are close to 120°, as one would expect for a ZnO single crystal. When very small areas within the large flat features were imaged, small ledges of approximately one or two atomic spacings in height are nearly always observed (see Fig. 1(C)). Based on these observations, we assumed that these macroscopically large flat regions are individual grains of ZnO, exposed to the tip in random orientations by the polishing procedure.

Tunneling spectra were acquired at many points on the surface, and a spectrum that is characteristic of the ZnO grains is shown in Fig. 2. This spectrum agrees qualitatively with parallel measurements performed on single-crystal ZnO polar and nonpolar faces. We have assigned the peaks labeled E_v and E_c to be the valence and conduction band edges, respectively, because the band edges of these peaks are close to the

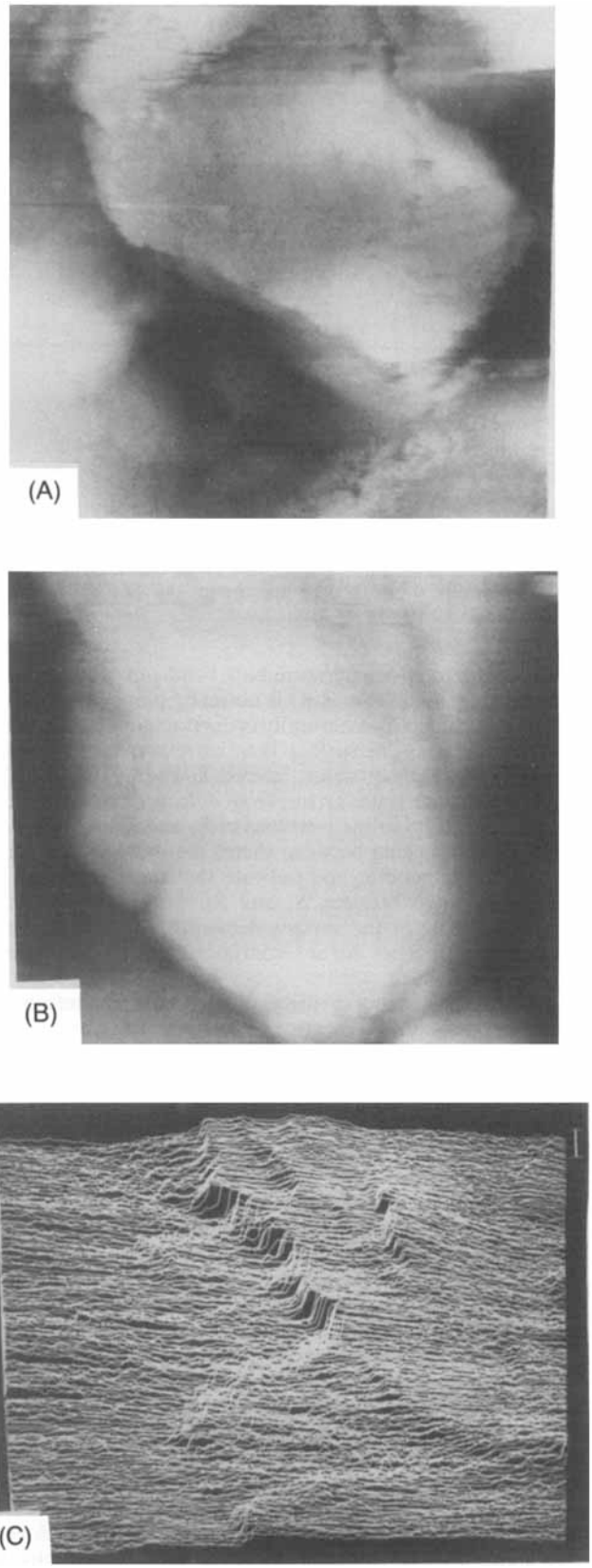

Fig. 1. Constant-current STM images of polycrystalline ZnO surfaces in UHV. (A) 495 nm × 495 nm (4950 Å × 4950 Å) gray-scale top-view image acquired using the conditions 0.5-nA and −2.75-V sample bias; height increases from black to white, the total height is 70 nm (700 Å). (B) 550 nm × 520 nm (5500 Å × 5200 Å) gray-scale top-view image acquired using the conditions 0.5-nA and −3.0-V sample bias; total height is 76 nm (760 Å). (C) 13.7 nm × 13.7 nm (137 Å × 137 Å) profile image acquired using the conditions 0.2-nA and −1.5-V sample bias; small scale bar in the upper righthand corner marks a height of 1.4 nm (14 Å).

[‡]The tip was ramped toward the sample at a rate of 0.07 nm (0.7 Å) per volt as the bias was increased from −3 to 0 V and then away from the sample at the same rate as the bias was increased to 3.0 V. The measured current was normalized assuming the barrier height to be 4.0 eV.

[¶]The "apparent" barrier height was computed in the normal way, assuming that the barrier, $\phi = [\Delta(\ln I)/1.025\Delta S(m^*)^{1/2}]^2$, where I is the tunnel current, S is the sample-tip separation, and m^* is the electron effective mass.

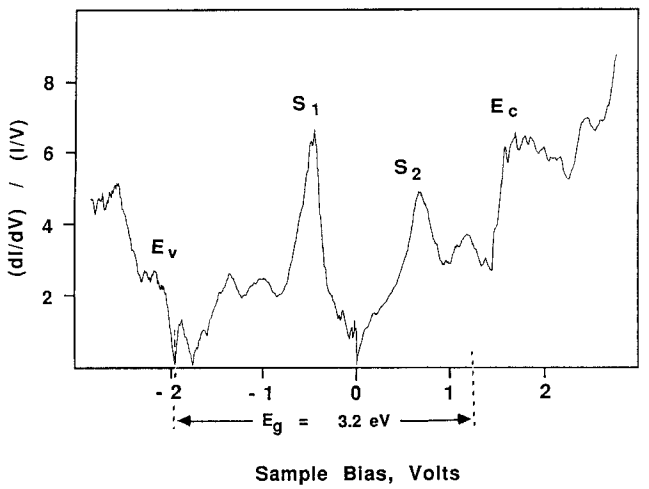

Fig. 2. Typical tunneling spectrum of the polycrystalline ZnO surface. Tip was ramped toward the sample at a rate of 0.07 nm/V (0.7 Å/V) as the bias increased from −3.0 to 0 V and then ramped away from the sample at the same rate as the bias increased toward 3.0 V. Markers showing the bulk energy gap of ZnO have been added to the horizontal axis.

value of the room-temperature bulk band gap of ZnO, 3.2 eV. The bulk Fermi level in ZnO is normally pinned near the top of the energy gap by a naturally occurring population of shallow donor states. The surface Fermi level, however, is pinned between two midgap states, labeled S_1 and S_2, which we assume are surface states arising from defects or contamination. Occasional shifts in the positions of E_v and E_c of up to 0.4 V (but not the spacing between them) are undoubtedly caused by local band bending and indicate that there is a small surface energy gap between S_1 and S_2. Imaging and spectroscopic mapping of the surface demonstrates that changes in electronic properties are sometimes correlated to features on the sample surface.

Figure 3(A) shows a three-dimensional rendering of a boundary region between two exposed grains, and Fig. 3(B) shows a gray-scale top-view image of the same area. A spike, labeled "S" in the upper part of the figure, is due to a tip instability and is not related to the sample surface. The feature of interest, a depression which varies in depth (maximum of ≈20 nm (≈200 Å)) and crosses the image at approximately a 45° angle, is indicated by the darker shades of gray. The arrows on Fig. 3(B) indicate the line along which the *I–V* curves were acquired and the numbers indicate the origins of the selected *I–V* curves shown in Figs. 3(C) to (G). The *I–V* curves clearly demonstrate that the conductivity in the depressed region is lower than that in the flat regions. Therefore, this is not simply a topographic feature, but rather a region where the electronic properties change, and, as a result of this, the contrast on the image contains a contribution from the lower conductivity in this area. Figure 4 demonstrates this point more clearly. The current recorded at −2 V is taken from each of the *I–V* curves acquired along the line indicated by the arrows and displayed as a function of distance across the image. The current, which reaches a minimum at the center of the grain boundary, is proportional to the conductivity and related to the integral of the density of states between the Fermi level and −2 V.

Four tunneling spectra are shown in Fig. 5, two of which were obtained outside the grain boundary (Figs. 5(A) and (D), which correspond to points labeled 1 and 5 on Fig. 3(B), respectively) and two which were obtained in the grain-boundary area (Figs. 5(B) and (C), which correpond to points 3 and 4 on Fig. 3(B), respectively). With the exception of an apparent gap region in the center of the spectra, an artifact of the limited dynamic range of spectra acquired at fixed sample-tip separations, these data compare favorably with those presented in Fig. 2. The most prominent difference between the spectra acquired near the grain boundary and those acquired far away is the width of the apparent gap in the center of the spectra. At points 1 and 5, the zero conductivity region is ≈0.65 eV wide, and at points 3 and 4, the region is ≈2 eV wide. Although the width of the zero conductivity region is essentially determined by an instrumental parameter, all of the spectra have been obtained under the same conditions and should therefore be comparable. The apparent absence of the states S_1 and S_2 is certainly one factor that contributes to observed decrease in total conductivity. It should be pointed out, however, that although these states were not detected, they still apparently exist because the Fermi level is still pinned near the center of the gap.

Figure 6(A) shows a three-dimensional representation of an STM image recorded on a different part of the same ZnO surface, and Fig. 6(B) is a gray-scale top-view of the same data which includes arrows to indicate the line along which I–V data were acquired. Beginning from the upper lefthand corner, the line first passes through a flat, featureless area, goes over a mound, and then back to a flat area. Continuing on, it passes over another mound and then into a crevice. Figure 6(C) clearly demonstrates that there is a correlation between the curent measured at −2.0 V during each *I–V* curve and the features on the image. Specifically, the current increases when the tip passes over each of the mounds and decreases in the crevice which we assume is a grain boundary. The same image and spectroscopic results have been obtained during three repetitions of this experiment.

Figure 7 shows four selected tunneling spectra from representative regions on the image. The tunneling spectra in Figs. 7(A) and (C) (from the points labeled 1 and 3 on the image) agree qualitatively with tunneling spectra acquired in the similar flat regions of Fig. 3, and the spectrum in Fig. 7(D) (from the area labeled 4) is similar to those obtained in the grain-boundary region of Fig. 3. The zero-conductivity region is again wider in the grain-boundary area. The tunneling spectrum in Fig. 6(B) was taken at the point labeled 2 on the image and is representative of the spectra acquired in the raised regions. These regions have a much higher conductivity than that of the rest of the surface, and only a very small conductivity gap occurs in the tunneling spectra. In addition, the tunneling spectra are not typical of those normally observed on these surfaces.

IV. Discussion

Images and spectroscopic maps have been used to identify three characteristic regions on the polycrystalline ZnO surface. First are the characteristic flat background areas that are normally observed on more than 90% of the surface and must correspond to random exposed faces of individual ZnO grains. Because the average grain size in this material is between 500 and 1000 nm (5000 and 10 000 Å), and the maximum area that can be imaged by STM is about 550 nm × 550 nm (5500 Å × 5500 Å), one would expect to observe only one individual grain or some portion of several grains in a single field of view. As expected, nearly every image of a large area contained a feature resembling a grain boundary, if not an entire grain. Therefore, the estimated size of the large flat regions agrees well with the known grain size and supports the conclusion that the flat areas are individual grains. The faceting of the large flat areas, which is observed in some images, provides additional supporting evidence, as does the similarity of the *I–V* spectra from these areas and clean, single-crystal ZnO surfaces.

On the other hand, spectroscopic data from the second of the characteristic regions do not agree with those acquired from other areas. Such high-conductivity areas, which appear as elevated areas on Fig. 6, show "metallic" spectral charac-

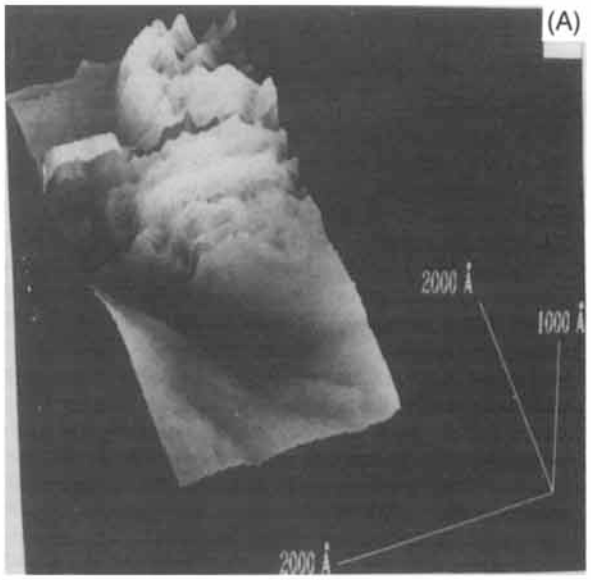

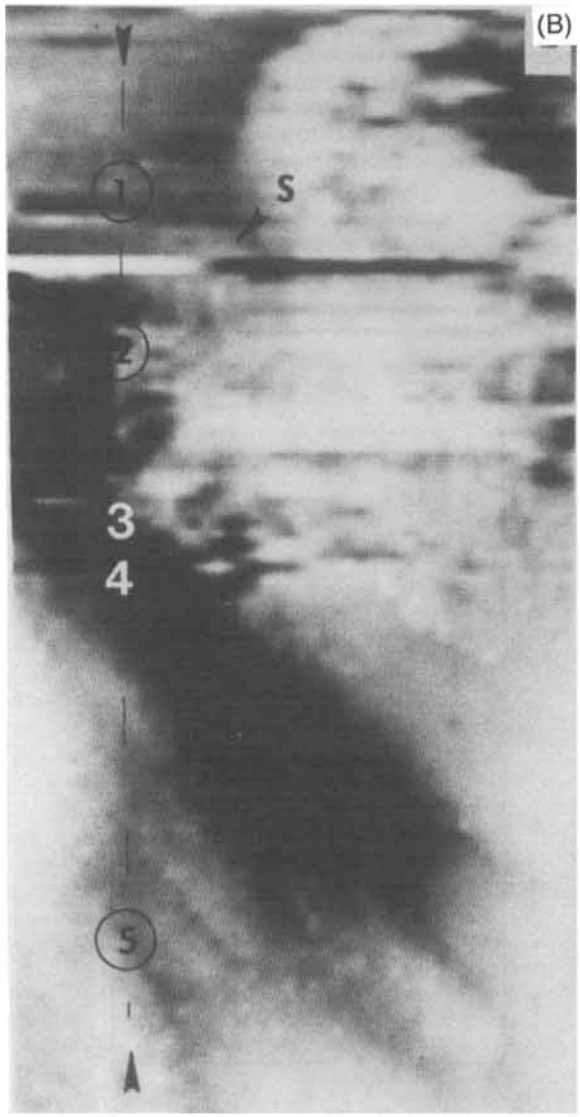

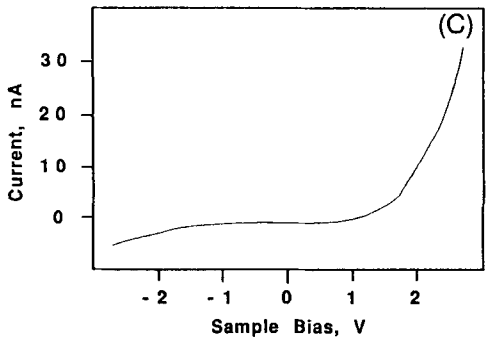

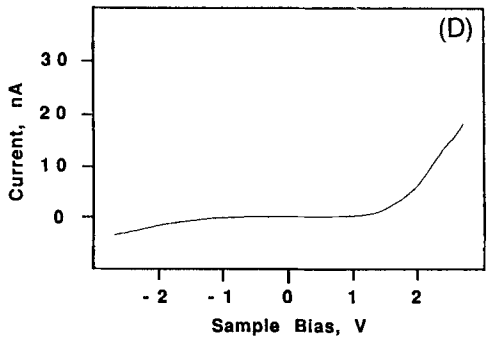

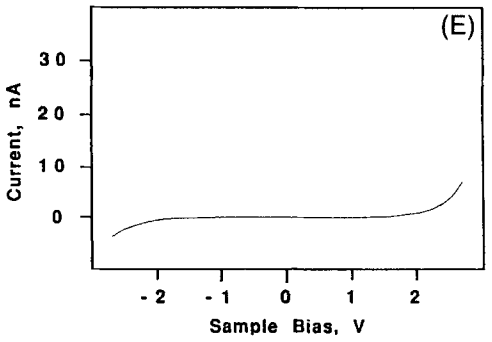

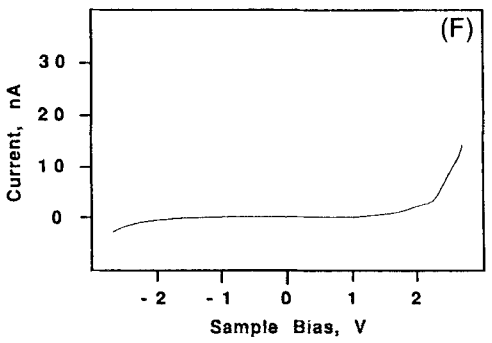

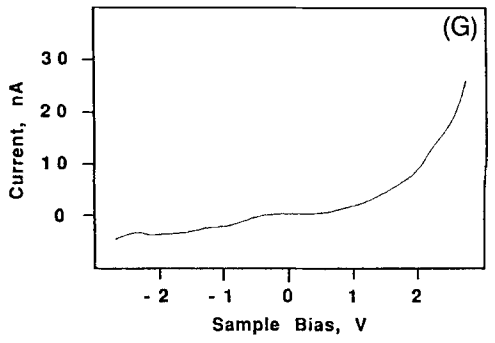

Fig. 3. (A) Three-dimensional rendering of a 200 nm × 400 nm (2000 Å × 4000 Å) image of a grain-boundary region; total height of the image is 40 nm (400 Å). (B) Gray-scale top-view rendering of the same image. Arrows at the top and bottom of the image indicate the line along which the *I–V* curves were acquired. Feature labeled "S" is a spike due to a temporary tip instability and is not related to the sample surface. Positions numbered 1 to 5 indicate the locations at which the *I–V* curves in Figs. 3(C) to (G) were acquired, respectively.

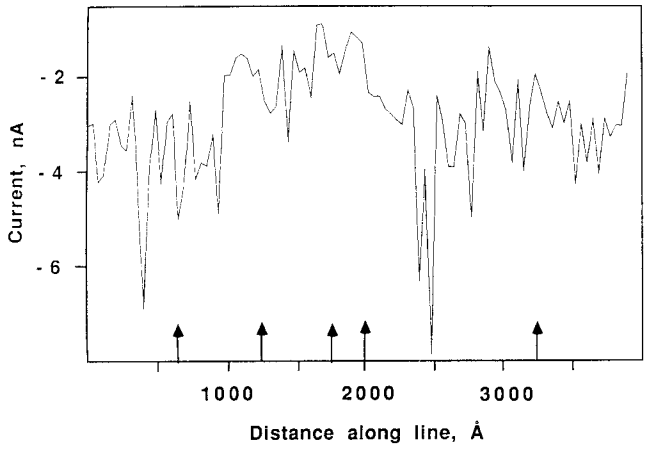

Fig. 4. Current measured at −2 V and the same sample-tip separation is plotted versus position along the line indicated in Fig. 3(B). Each of these data were taken from the *I–V* curves that were acquired along this line. The arrows mark the positions at which the *I–V* curves in Fig. 3 were acquired.

tersitics and, most likely, are not ZnO. One possibility is that they are one of the minority phases that are known to occur in these sintered materials.[11,12] Another possibility is that these are areas of surface contamination, perhaps by carbon. This seems especially likely in view of the amorphous shape of the area, the high conductivity, and the known presence of carbon. At this time, however, there is insufficient evidence to distinguish between these possibilities. Some portion of the contrast in the STM image in these regions is certainly due to the increased conductivity. The detection of this "impurity" is not possible by imaging alone and demonstrates the importance of spectroscopic mapping when analyzing inhomogeneous materials.

The most exciting of the observations are the low-conductivity regions that separate the large flat areas and appear as topographic depressions in images. These features, which are the third characteristic region of these surfaces, have the size, shape, and expected electronic properties of ZnO grain boundaries. According to the widely accepted model for a ZnO grain boundary, the carrier concentration near a grain boundary is reduced by local band bending. Flores and Garcia[17] have shown that a decreased carrier concentration leads to an increased resistance near a metal–semiconductor tunnel junction. The increased resistance would lead, in turn, to lower tunnel currents at a given bias and sample-tip separation, an effect clearly demonstrated in Figs. 3 and 6(C), which show that regions of increased resistance are detected several tens of nanometers (hundreds of angstroms) on both sides of the boundary. The observations also indicate that the widths of the depletion layers, ≈80 nm (≈800 Å) at the widest part of Fig. 3(B) and ≈40 nm (≈400 Å) at the widest part of Fig. 6(B), are not the same in all cases. Such variations may be due to local differences in the composition of the interfacial region. The observed range in widths of the depletion layers is consistent with calculations using typical values for the interface barrier height and bulk donor density.[11]

Estimates of the amount of band bending at these interfaces vary from one-half to several electron volts, depending on the experimental technique used to measure it.[11] Although

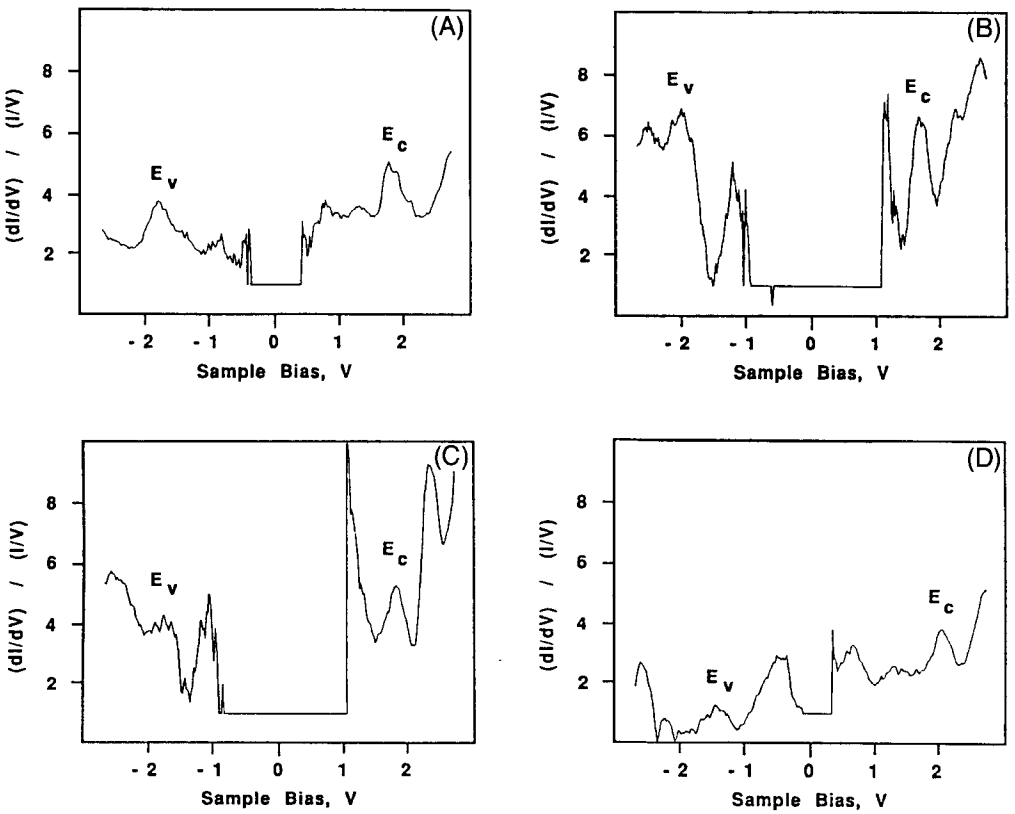

Fig. 5. Four tunneling spectra computed from four representative *I–V* curves in Fig. 3. (A) and (D) correspond to positions 1 and 5, respectively, and (B) and (C) correspond to positions 3 and 4, respectively. In each case, the peaks assigned to the valance and conduction band have been labeled E_v and E_c, respectively.

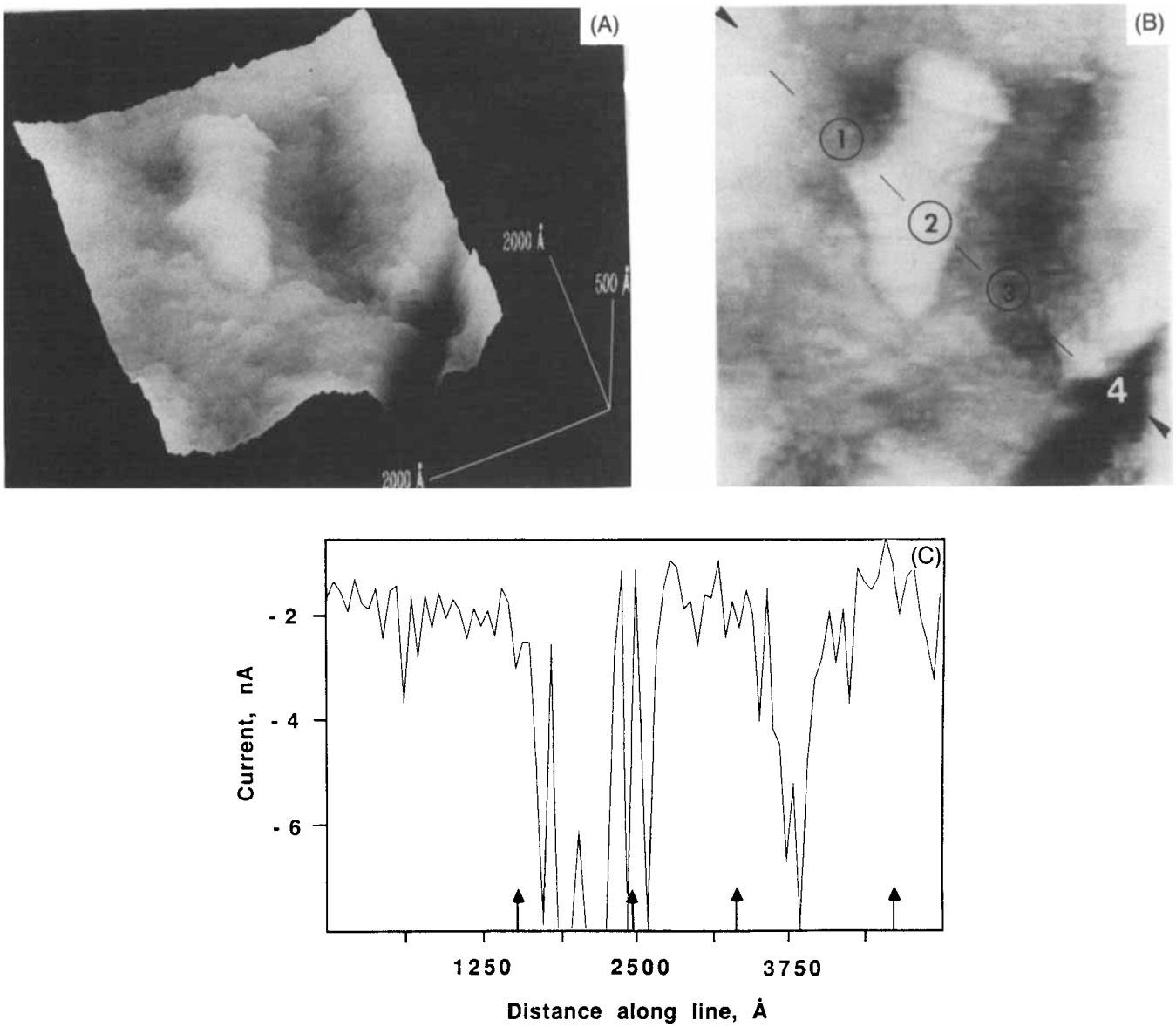

Fig. 6. (A) Three-dimensional rendering of a 350 nm × 400 nm (3500 Å × 4000 Å) image of a ZnO surface showing several features of interest; the total height of the image is 45 nm (450 Å). (B) Gray-scale top-view rendering of the same image; arrows at the top-left and bottom-right corners of the image indicate the diagonal line along which the *I–V* curves were acquired and positions numbered 1 to 4 indicate the locations at which the *I–V* curves in Figs. 7(A) to (D) were acquired, respectively. (C) Current measured at −2 V and the same sample-tip separation plotted versus position along the line indicated in Fig. 6(B). Each of these data were taken from the *I–V* curves that were acquired along this line. Arrows mark the positions at which the *I–V* curves were acquired.

the measurements presented here demonstrate local band-bending effects of up to 0.4 eV (for example, note the position of E_c and E_v in Fig. 4(A) relative to the positions in Fig. 4(B)), there is no apparent systematic correlation of these effects with the position of the grain boundary. However, it is not expected that bulk band bending would be observed as shifts in spectral peak positions, because the surface Fermi level is pinned by the surface states S_1 and S_2. The small band-bending effects, which are detected as shifts in the spectra, appear to be rather local in their lateral extent and may therefore be due to localized surface phenomena and not representative of the bulk.[16] However, because some fraction of the voltage between the tip and the semiconductor surface also drops the semiconductor bulk, the experiment is still sensitive to changes in bulk properties such as the increase in resistance and decrease in bulk charge carrier density that are expected to be associated with grain boundaries. There are actually two superimposed depletion layers at the surface, a situation depicted schematically in Fig. 8. The first is the nearly constant space-charge region due to the flow of the tunneling current which surrounds the tip at all times. It is this voltage drop that allows the tunneling experiment to probe the subsurface electrical properties of ZnO. The space-charge region caused by the grain boundary, on the other hand, varies with position depending on the proximity to such an interface. Therefore, the fixed depletion layer in the bulk, associated with a grain boundary, is simply detected as an area of increased resistance in the tunneling spectra.

V. Conclusion

We have demonstrated that scanning tunneling microscopy (STM) analysis, including spatially resolved tunneling spectroscopy, can be used to detect local variations in the electrical properties of polycrystalline materials such as ZnO varistors. In fact, the spectroscopic "mapping" of an inhomogeneous surface is necessary to determine whether contrast arises from geometric or electronic sources. Tunneling spectroscopy was used to identify individual grains, grain boundaries, and surface impurities. The fact that a portion of

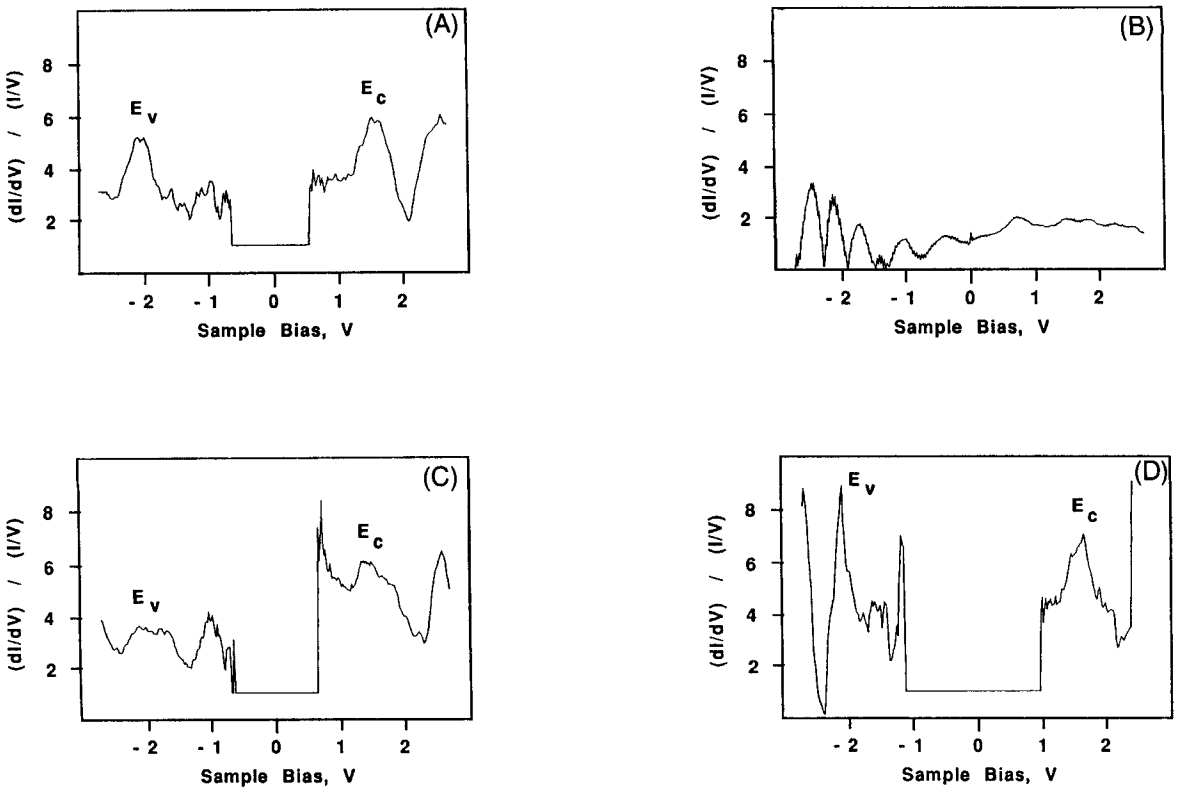

Fig. 7. Four tunneling spectra computed from *I–V* curves acquired at the locations labeled 1 to 4 in Fig. 6. Figures 7(A) to (D) correspond to 1 to 4, respectively. In the case of Figs. 7(A), (C), and (D), the peaks assigned to the valance and conduction band have been labeled E_v and E_c, respectively.

the applied voltage is dropped in a space-charge layer in the semiconductor allows some "bulk" properties to be probed. In this case, grain boundaries, which show up topographically as depressions on the image, were detected as areas of increased resistance using tunneling spectroscopy. Thus, this is a promising technique for the study of individual interfaces, and we anticipate that the further development of this technique will lead to a more complete description of the electrical properties and charge state of a variety of interfaces and grain boundaries.

Acknowledgments: We are grateful to G. Pike at Sandia National Laboratories for providing ZnO samples and to J. Vohs for valuable discussions and for providing ZnO single crystal. Technical assistance from I. Solomon is also appreciated.

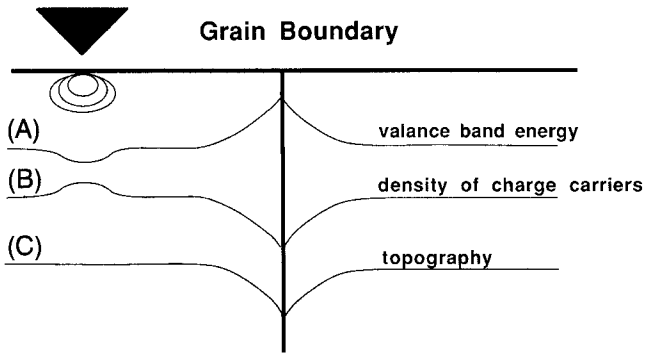

Fig. 8. When tunneling on a semiconductor, some of the bias applied to the tunnel junction is dropped in a space charge region in the semiconductor bulk that follows the tip. In the situation depicted here, the tip has a positive charge and the grain boundary has a negative interfacial charge: (A) local band bending near the tip and near a grain boundary, (B) local charge carrier density, and (C) topographic signal.

References

[1]G. Binning, H. Rohrer, Ch. Gerber, and E. Weibel, "Surface Studies by Scanning Tunneling Microscopy," *Phys. Rev. Lett.*, **49**, 57 (1982).

[2]G. Binning, H. Rohrer, Ch. Gerber, and E. Stoll, "Real-Space Observation of the Reconstruction of Au(100)," *Surf. Sci.*, **144**, 321 (1984).

[3]R. M. Feenstra, J. A. Stroscio, and A. P. Fein, "Tunneling Spectroscopy of the Si(111)2×1 Surface," *Surf. Sci.*, **181**, 295 (1987).

[4]R. J. Hamers and J. E. Demuth, "Electronic Structure of Localized Si Dangling-Bond Defects by Tunneling Spectroscopy," *Phys. Rev. Lett.*, **60**, 2527 (1988).

[5]J. K. Gimzewski, A. Humbert, D.W. Pohl, and S. Veprek, "Scanning Tunneling Microscopy of Nanocrystalline Silicon Surfaces," *Surf. Sci.*, **168**, 795 (1986).

[6]O. Nishikawa and M. Tomitori, "Scanning Tunneling Microscopy Study of Conductive Ceramics," *J. Vac. Sci. Technol.*, **A6**, 454 (1988).

[7]N. J. Zheng, U. Knipping, I. S.T. Tsong, W.T. Petuskey, and J. C. Barry, "Scanning Tunneling Microscopy of *b*-SiC and $YBa_2Cu_3O_{7-x}$ Ceramic Surfaces," *J. Vac. Sci. Technol.*, **A6**, 457 (1988).

[8]J. R. Kirtly, S. Washburn, and M. J. Brady, "Scanning Tunneling Measurements of Potential Steps at Grain Boundaries in the Presence of Current Flow," *Phys. Rev. Lett.*, **60**, 1546 (1988).

[9]D. A. Bonnell and D. R. Clarke, "Scanning Tunneling Microscopy and Spectroscopy of Ceramics: Silicon Carbide and Zinc Oxide," *J. Am. Ceram. Soc.*, **71**, 629 (1988).

[10]D. A. Bonnell, "Characterization of Carbides by Scanning Tunneling Microscopy," *Mater. Sci. Eng.*, **A105/106**, 55 (1988).

[11]W. G. Morris, "Physical Properties of Electrical Barriers in Varistors," *J. Vac. Sci. Technol.*, **13**, 926 (1976).

[12]R. G. Dosch, B. A. Tuttle, and R. A. Brooks, "Chemical Preparation and Properties of High-Field ZnO Varistors," *J. Mater. Res.*, **1**, 90 (1986).

[13]G. S. Rohrer and D. Bonnell, "Probing the Surface Chemistry of Polycrystalline ZnO with Scanning Tunneling Microscopy and Tunneling Spectroscopy"; unpublished work.

[14]N. D. Lang, "Spectroscopy of Single Atoms in the Scanning Tunneling Microscope," *Phys. Rev. B*, **36**, 5947 (1986).

[15]J. P. Stroscio, R. M. Feenstra, and A. P. Fein, "Electronic Structure of the Si(111)2×1 Surface by Scanning-Tunneling Microscopy," *Phys. Rev. Lett.*, **57**, 2579 (1986).

[16]P. Martensson and R. M. Feenstra, "Geometric and Electronic Structure of Antimony on the GaAs(110) Surface Studied by Scanning Tunneling Microscopy," *Phys. Rev. B*, **39**, 7744 (1989).

[17]F. Flores and N. Garcia, "Voltage Drop in the Experiments of Scanning Tunneling Microscopy for Si," *Phys. Rev. B*, **30**, 2289 (1984). □